Supporting Information

of

Modeling Bi-directional Permeation of Electrolytes in Osmotically Driven Membrane Processes

Nathan T. Hancock[1], William A. Phillip [2]*, Menachem Elimelech[3], Tzahi Y. Cath[1]*

[1] Division of Environmental Science and Engineering
1500 Illinois Street
Colorado School of Mines
Golden, Colorado 80401

[2]Department of Chemical and Biomolecular Engineering
182 Fitzpatrick Hall
University of Notre Dame
Notre Dame, Indiana 46556-5637

[3]Department of Chemical and Environmental Engineering
P.O. Box 208286
Yale University
New Haven, Connecticut 06520-8286

*To whom correspondence should be addressed: wphillip@nd.edu, tcath@mines.edu

Revised: October 19, 2011

Submitted to *Environmental Science and Technology*

Contents:

S1. Derivation of uncoupled bidirectional solute permeation model

Considering the mass transfer of feed and draw solution (DS) solutes through the membrane independent from one another facilitates derivation of a predictive model for uncoupled bi-directional transport in osmotically driven membrane processes (ODMP). First we develop an analytical expression for the reverse solute flux of DS solutes into the support layer by writing a steady-state mass balance on a differential volume for the support layer

$$\frac{dJ_1^D}{dz} = -D^s \frac{d^2c_1}{dz} + J_w \frac{dc_1}{dz} = 0 \tag{1}$$

where D^s is the effective diffusion coefficient for the solute within the support layer, J_w is the superficial fluid velocity (which is equivalent to the water flux), and z is defined in Figure 1. Quantities written with superscript D convey that they are measured on the DS side of the active layer. Also note that this mass balance assumes that D^s, J_1^D, and J_w are independent of z and are constant across the entire support layer. The effective diffusion coefficient for the solute within the support layer is related to the bulk diffusion coefficient by accounting for the porosity and tortuosity of the support layer (*1, 2*)

$$D^s = \frac{D\varepsilon}{\tau} \tag{2}$$

The solution to the second order ordinary differential equation presented in Eq. 1 is

$$c_1 = C_1 + C_2 \exp\left(\frac{J_w \tau}{D\varepsilon} z\right) \tag{3}$$

where C_1 and C_2 are generic constants of integration, and are subjected to the following boundary conditions as illustrated in Figure 1a:

$$c_1(z=0) = c_1^{D,i} \tag{4a}$$

$$c_1(z=t_s) = c_1^{D,b} \tag{4b}$$

Combining Eqs. 3, 4a, and 4b yield an expression for the DS solute concentration profile in the porous support layer:

$$c_1(z) = \frac{\left(c_1^{D,b} - c_1^{D,i}\right)\exp\left(\frac{J_w S}{D} z\right) + c_1^{D,i} \exp\left(\frac{J_w S}{D}\right) - c_1^{D,b}}{\exp\left(\frac{J_w S}{D}\right) - 1} \tag{5}$$

Note that the derived equation for the concentration profile of the DS solute in the support layer contains the dimensionless Peclet number defined as the ratio of advection to the rate of diffusion for a quantity driven by an appropriate gradient (*3*)

$$Pe_1^D = \frac{J_w S}{D} \tag{6}$$

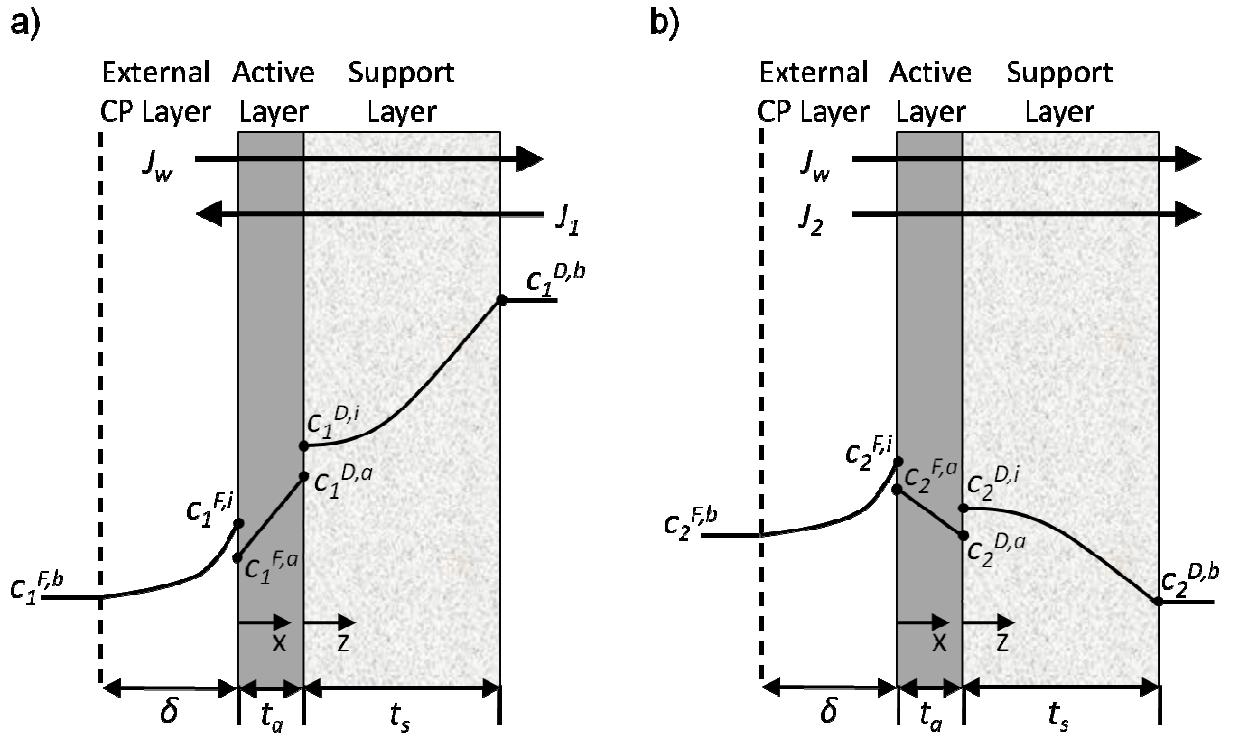

FIGURE 1: Schematics of concentration profiles for (a) the draw solution electrolyte and (b) the feed solution electrolyte. Local coordinates x and z are established with respect to the forward water flux (J_w). Both electrolytes are transported down their concentration gradient resulting in a net reverse flux of draw solution electrolyte, J_1, and a net forward flux of feed solution electrolyte, J_2. Electrolytes must be transported across the external concentration polarization layer, active layer, and porous support layer with thickness δ, t_a, and t_s, respectively. Subscripts are used to denote either the draw solution electrolyte (*1*) or feed solution electrolyte (*2*). Superscripts represent the concentration of these ions at specific locations along their concentration profile, where *F* and *D* correspond to the feed and draw solution sides of the active layer, and *b*, *i*, and *a* correspond to the bulk solution, interface, or active layer, respectively.

Flux of the DS solute through the support layer is equal to the sum of the diffusive and convective components of the flux:

$$J_1^D = -D\frac{dc_1}{dz} + J_w c_1 \tag{7}$$

Substituting Eq. 5 into Eq. 7 yields an expression for the DS solute flux through the support layer

$$J_1^D = J_w\left(\frac{c_1^{D,i}\exp\left(Pe_1^s\right)-c_1^{D,b}}{\exp\left(Pe_1^s\right)-1}\right) \tag{8}$$

As written, Eq. 8 uses the DS solute concentration at the interface, $c_1^{D,i}$, which cannot be measured. Additional effort is required to formulate a solution that utilizes experimentally accessible parameters.

Next a steady-state mass balance across the active layer is considered:

$$\frac{dJ_1^a}{dx} = -D^a\frac{d^2c_1}{dx^2} = 0 \tag{9}$$

where D^a is the average diffusion coefficient for the electrostatically coupled DS cation and anion within the active layer. The solution to this second order ordinary differential equation is given by

$$c_1 = C_1 + C_2x \tag{10}$$

subject to the following boundary conditions as illustrated in Figure 1a

$$c_1\left(x=0\right) = c_1^{F,a} \tag{11a}$$

$$c_1\left(x=t_a\right) = c_1^{D,a} \tag{11b}$$

Combining Eq. 10 through 11b yield an expression for the DS solute concentration profile in the active layer:

$$c_1\left(x\right) = c_1^{F,a} + \left(c_1^{D,a} - c_1^{F,a}\right)\frac{x}{t_a} \tag{12}$$

Solution-diffusion theory dictates that flux of the DS solute through the active layer is only equal to the diffusive flux component

$$J_1^a = -D^a\frac{dc_1}{dx} \tag{13}$$

Substituting Eq. 12 into Eq. 13 yields an expression for the DS solute flux through the active layer

$$J_1^a = -\frac{D^a}{t_a}\left(c_1^{D,a} - c_1^{F,a}\right) \tag{14}$$

The concentration of the DS solute at the interior interfaces of the active layer are related to the DS solute concentration at the interfaces exterior to the active layer by

$$c_1^{D,a} = Hc_1^{D,i} \tag{15a}$$

$$c_1^{F,a} = Hc_1^{F,i} \tag{15b}$$

Substitution of Eqs. 15a and 15b into Eq. 14 provides an expression for the flux of the DS solute through the active layer in terms of the solute concentrations at the exterior interfaces of the active layer

$$J_1^a = -B_1\left(c_1^{D,i} - c_1^{F,i}\right) \tag{16}$$

One additional mass balance is required to describe flux of the DS solute into the active layer. A steady-state mass balance across the external concentrative CP boundary layer on the feed (*F*) side of the active layer yields:

$$\frac{dJ_1^F}{dx} = -D\frac{d^2c_1}{dx^2} + J_w\frac{dc_1}{dx} = 0 \tag{17}$$

The solution to this second order ordinary differential equation is similar to Eq. 3

$$c_1 = C_1 + C_2\exp\left(\frac{J_w}{D}x\right) \tag{18}$$

and is subject to the following boundary conditions as illustrated in Figure 1a

$$c_1\left(x=0\right) = c_1^{F,i} \tag{19a}$$

$$c_1\left(x=-\delta\right) = c_1^{F,b} \tag{19b}$$

where δ is the thickness of the concentration boundary layer over which the concentration deviates from the bulk feed concentration and is derived from film theory (*4-7*)

$$\delta = \frac{d_h}{Sh} \tag{20}$$

where d_h is the hydraulic diameter calculated for a rectangular cross section flow cell and *Sh* is the dimensionless Sherwood number that is proportional to the product of the Reynolds number and the Schmidt number (*5, 6*).

Combining Eqs. 18 through 19b yield the concentration profile of the DS solute in the concentrative external CP layer

$$c_1\left(x\right) = \frac{\left(c_1^{F,b} - c_1^{F,i}\right)\exp\left(\frac{J_w}{D}x + \frac{J_w d_h}{ShD}\right) - c_1^{F,b}\exp\left(\frac{J_w d_h}{ShD}\right) + c_1^{F,i}}{1-\exp\left(\frac{J_w d_h}{ShD}\right)} \tag{21}$$

The derived equation for the concentration profile of the DS solute in the CP boundary layer contains a second dimensionless Peclet number, similar to Eq. 6

$$Pe_1^F = \frac{J_w d_h}{ShD} = \frac{J_w}{\kappa} \tag{22}$$

where κ is the transfer coefficient calculated for a rectangular cross section flow cell.

Flux of the DS solute through the CP boundary layer is equal to the sum of the diffusive and convective components of the flux

$$J_1^F = -D\frac{dc_1}{dx} + J_w c_1 \tag{23}$$

Substituting Eq. 21 into Eq. 23 yields an expression for the DS solute flux through the CP boundary layer on the feed side of the membrane

$$J_1^F = J_w\left(\frac{c_1^{F,i} - c_1^{F,b}\exp\left(Pe_1^F\right)}{1-\exp\left(Pe_1^F\right)}\right) \tag{24}$$

Assuming that at steady-state there is no net accumulation and no reaction of the DS solute at either the feed – active layer interface (x=0) or active layer – support layer interface (z=0), a final set of mass balances yield

$$J_1^F\left(x=0\right) = J_1^a\left(x=0\right) \tag{25a}$$

$$J_1^D\left(z=0\right) = J_1^a\left(z=0\right) \tag{25b}$$

Thus, the final expression for the reverse flux of the DS solute through the asymmetric membrane shown in Figure 1a is

$$J_1 = \frac{J_w B_1\left(c_1^{F,b}\exp\left(Pe_1^F + Pe_1^D\right) - c_1^{D,b}\right)}{\left(B_1\exp\left(Pe_1^F\right) + J_w\right)\exp\left(Pe_1^D\right) - B_1} \tag{26}$$

A similar series of mass balances following the same set of assumptions listed in the derivation of Eq. 26 produces an expression for the forward flux of a feed solute through the asymmetric membrane shown in Figure 1b

$$J_2 = \frac{J_w B_2\left(c_2^{F,b}\exp\left(Pe_2^F + Pe_2^D\right) - c_2^{D,b}\right)}{\left(B_2\exp\left(Pe_2^F\right) + J_w\right)\exp\left(Pe_2^D\right) - B_2} \tag{27}$$

written in this form, Eqs. 26 and 27 can be used with experimentally accessible parameters to predict the permeation of both feed and DS solutes through an asymmetric membrane in FO mode.

Nomenclature

B	solute permeability coefficient
C	constant of integration
c	molar concentration of solute
D	bulk diffusion coefficient of solute in water
d_h	hydraulic diameter of a rectangular channel
H	solute partition coefficient
J_s	molar solute flux
J_w	water flux
S	membrane structural parameter
t_a	thickness of active layer
t_s	thickness of support layer
x, z	local coordinate system
δ	thickness of external CP layer
ε	porosity of support layer
ϕ	electrostatic potential
κ	external mass transfer coefficient
τ	tortuosity of support layer

S2. Molar solute fluxes from solute permeability experiments

Table S1: Mass transfer rates measured during PRO-mode experiments and salt permeance coefficient calculated for all salts used during this investigation. Salt pairs are listed in order from most chaotropic to most kosmotropic based on their anion (*8*).

Salt	**Cation flux, mmol/m^2·hr**	**Anion flux, mmol/m^2·hr**	***B*, 10^{-8} m/s**
$NaClO_4$	1297.8 ± 21.7	1295.5 ± 9.9	49.92
KNO_3	556.0 ± 11.2	562.5 ± 17.3	20.42
$NaNO_3$	420.5 ± 10.1	433.3 ± 15.4	16.28
$Ca(NO_3)_2$	74.5 ± 1.5	146.2 ± 3.4	5.04
KBr	400.0 ± 4.3	411.2 ± 4.1	16.19
NaBr	288.0 ± 2.8	288.3 ± 1.6	12.56
KCl	190.4 ± 0.2	191.8 ± 3.0	7.64
NaCl	156.7 ± 7.7	155.1 ± 0.5	6.02
$CaCl_2$	33.7 ± 0.7	64.2 ± 0.6	2.38
$SrCl_2$	27.4 ± 1.8	56.1 ± 1.1	1.99
KH_2PO_4	18.3 ± 4.4	18.2 ± 2.1	1.26
Na_2SO_4	30.5 ± 2.9	15.8 ± 0.2	1.72
$MgSO_4$	2.8 ± 0.3	3.0 ± 0.3	0.11

S3. Summary of water flux, solute flux, and experimental error from ternary experiments

Table S2: Summary of common anion experiments with the more mobile cation in the DS.

Experiment (DS-feed)	**Chemical species**	**Observed Salt Concentration, M**	**Average net J_s, mmol/m^2·hr**	**J_w, 10^{-6} m/s**	**Apparent current[*] I=$\sum z \cdot J_s$, meq/m^2·hr**
KCl-NaCl	K^+	0.93	134.0	2.83	2.8
	Cl^-		124.5		
	Na^+	0.05	12.3		
KCl-$CaCl_2$	K^+	0.93	122.0	2.68	-4.6
	Cl^-		110.4		
	Ca^{2+}	0.05	3.5		
KBr-NaBr	K^+	0.95	226.6	2.88	-3.2
	Br^-		207.6		
	Na^+	0.05	15.8		
KCl-$SrCl_2$	K^+	0.96	132.5	2.67	0.5
	Cl^-		129.8		
	Sr^{2+}	0.05	1.6		
KNO_3-$NaNO_3$	K^+	0.95	390.4	2.41	3.0
	NO_3^-		373.0		
	Na^+	0.05	20.3		

[*] Calculating the apparent current based on ion flux data is an unambiguous method to validate overall mass transport behavior observed during experiments. A value of zero is expected for ODMP where no electrical current is applied. Values deviating from zero are caused by experimental or analytical error.

Table S3: Summary of common anion experiments with the more mobile cation in the feed.

Experiment (DS-feed)	**Chemical species**	**Observed Salt Concentration, M**	**Average net J_s, mmol/m^2·hr**	**J_w, 10^{-6} m/s**	**Apparent current[*] $I=\sum z \cdot J_s$, meq/m^2·hr**
NaCl-KCl	Na^+	0.90	98.5	2.63	4.0
	Cl^-		83.3		
	K^+	0.05	11.2		
$CaCl_2$-KCl	Ca^{2+}	0.98	19.3	2.85	-0.2
	Cl^-		31.4		
	K^+	0.05	6.9		
NaBr-KBr	Na^+	0.90	139.0	2.60	4.78
	Br^-		131.9		
	K^+	0.05	11.9		
$SrCl_2$-KCl	Sr^{2+}	0.97	14.8	2.50	-0.5
	Cl^-		22.6		
	K^+	0.05	6.6		
$NaNO_3$-KNO_3	Na^+	0.95	253.0	2.41	9.37
	NO_3^-		240.5		
	K^+	0.05	21.8		

[*] Calculating the apparent current based on ion flux data is an unambiguous method to validate overall mass transport behavior observed during experiments. A value of zero is expected for ODMP where no electrical current is applied. Values deviating from zero are caused by experimental or analytical error.

Table S4: Summary of common cation experiments excluding experiments that contain nitrate.

Experiment (DS-feed)	**Chemical species**	**Observed Salt Concentration, M**	**Average net J_s, mmol/m^2·hr**	**J_w, 10^{-6} m/s**	**Apparent current[*] $I=\sum z \cdot J_s$, meq/m^2·hr**
KCl-KH_2PO_4	K^+	0.98	150.3	2.80	2.72
	Cl^-		161.3		
	$H_2PO_4^-$	0.06	8.3		
$NaCl$-$NaClO_4$	Na^+	0.94	16.3	2.40	2.35
	Cl^-		123.4		
	ClO_4^-	0.05	104.8		
$NaClO_4$-$NaCl$	Na^+	0.93	636.5	2.04	1.02
	ClO_4^-		648.3		
	Cl^-	0.05	10.8		
$NaCl$-Na_2SO_4	Na^+	0.95	96.3	2.04	-2.27
	Cl^-		107.8		
	SO_4^{2-}	0.05	6.7		

[*] Calculating the apparent current based on ion flux data is an unambiguous method to validate overall mass transport behavior observed during experiments. A value of zero is expected for ODMP where no electrical current is applied. Values deviating from zero are caused by experimental or analytical error.

Table S5: Summary of common cation experiments with salts that contain nitrate.

Experiment (DS-feed)	**Chemical species**	**Observed Salt Concentration, M**	**Average net J_s, mmol/m^2·hr**	**J_w, 10^{-6} m/s**	**Apparent current* $I=\sum z \cdot J_s$, meq/m^2·hr**
$CaCl_2$-$Ca(NO_3)_2$	Ca^{2+}	0.96	5.6	2.60	6.28
	Cl^-		158.3		
	NO_3^-	0.05	140.7		
$Ca(NO_3)_2$-$CaCl_2$	Ca^{2+}	0.92	35.6	2.42	1.45
	NO_3^-		199.8		
	Cl^-	0.05	127.0		
NaCl-$NaNO_3$	Na^+	0.95	32.0	2.60	-3.17
	Cl^-		173.6		
	NO_3^-	0.05	144.8		
$NaNO_3$-NaCl	Na^+	0.92	233.7	2.42	1.30
	NO_3^-		311.3		
	Cl^-	0.05	76.4		

* Calculating the apparent current based on ion flux data is an unambiguous method to validate overall mass transport behavior observed during experiments. A value of zero is expected for ODMP where no electrical current is applied. Values deviating from zero are caused by experimental or analytical error.

S4. Molar flux of potassium as a function of $CaCl_2$ concentration

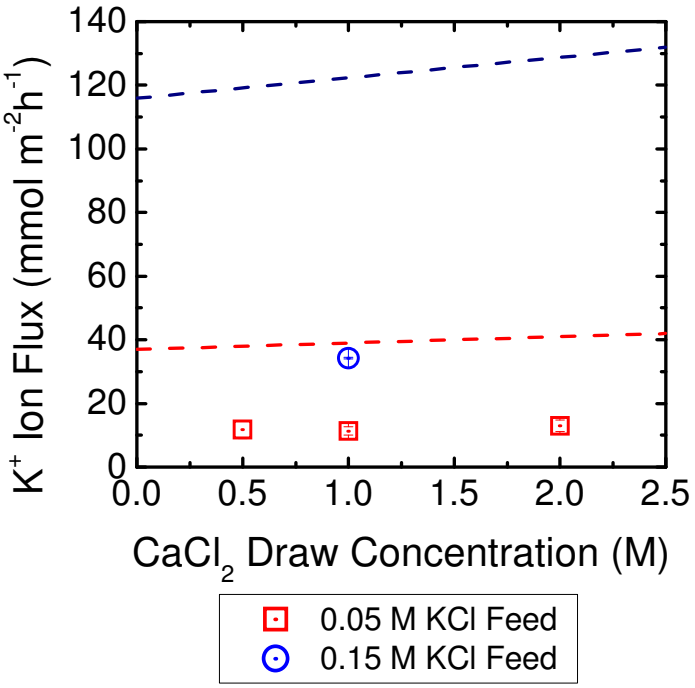

FIGURE S1: Feed ion flux as a function of draw solution concentration. The experimental potassium ion flux was measured for several different $CaCl_2$ draw solution concentrations. In addition, the potassium ion flux was determined at two different feed solution concentrations, 0.05 and 0.15 M KCl, for a 1.0 M $CaCl_2$ draw solution concentration. The dashed lines represent the predicted potassium flux using Eq. 2. As a result of concentration polarization, a slight increase in potassium ion flux is predicted because higher $CaCl_2$ concentrations generate higher water fluxes. The transport parameters D, B, and k correspond to those reported in Table 1 for Membrane II, and S = 559 μm. Error bars represent one standard deviation.

S5. Summary of water flux, solute flux, and experimental error from quaternary experiments

Table S6: Summary of measured quantities from quaternary experiments.

Experiment (DS-feed)	**Chemical species**	**Observed Salt Concentration, M**	**Average J_s, mmol/m^2·hr**	**J_w, 10^{-6} m/s (std. deviation)**	**Apparent current* $I=\sum z \cdot J_s$, meq/m^2·hr**
$NaCl$-$MgSO_4$	Na_+	0.97	94.0	2.65 (0.43)	1.24
	Cl^-		97.3		
	Mg^{2+}	0.05	0.6		
	SO_4^{2-}		1.6		
$NaCl$-KNO_3	Na_+	0.93	65.5	2.45 (0.43)	-1.51
	Cl^-		150.6		
	K^+	0.05	29.9		
	NO_3^-		116.5		
$MgSO_4$-KNO_3	Mg^{2+}	0.93	2.4	1.10 (0.39)	2.94
	SO_4^{2-}		5.2		
	K^+	0.05	31.8		
	NO_3^-		34.5		
$NaCl$-K_2SO4	Na_+	0.84	59.3	2.25	-3.87
	Cl^-		61.3		
	K^+	0.01	3.6		
	SO_4^{2-}		0.9		

* Calculating the apparent current based on ion flux data is an unambiguous method to validate overall mass transport behavior observed during experiments. A value of zero is expected for ODMP where no electrical current is applied. Values deviating from zero are caused by experimental or analytical error.

Literature Cited

(1) Dullien, F. A. L., *Porous media: fluid transport and pore structure*. 2nd ed. ed.; Academic Press: Sand Diego, 1992.

(2) Cussler, E. L., *Diffusion mass transfer in fluid systems*. 3rd ed. ed.; University Press: Cambridge, 2009.

(3) Bird, R. B.; Stewart, W. E.; Lightfoot, E. N., *Transport Phenomena*. 2nd ed.; John Wiley & Sons, Inc.: 2007.

(4) Zydney, A. L., Stagnant film model for concentration polarization in membrane systems. *Journal of Membrane Science* **1997,** *130*, (1-2), 275-281.

(5) Hoek, E. M. V.; Kim, A. S.; Elimelech, M., Influence of Crossflow Membrane Filter Geometry and Shear Rate on Colloidal Fouling in Reverse Osmosis and Nanofiltration Separations. *Environmental Engineering Science* **2002,** *19*, (6), 357-372.

(6) McCutcheon, J. R.; Elimelech, M., Influence of concentrative and dilutive internal concentration polarization on flux behavior in forward osmosis. *Journal of Membrane Science* **2006,** *284*, (1-2), 237-247.

(7) Sablani, S. S.; Goosen, M. F. A.; Al-Belushi, R.; Wilf, M., Concentration polarization in ultrafiltration and reverse osmosis: A critical review. *Desalination* **2001,** *141*, 269-289.

(8) Zhang, Y.; Cremer, P. S., Interactions between macromolecules and ions: the Hofmeister series. *Current Opinion in Chemical Biology* **2006,** *10*, 658-663.